

Dynamic stability of a viscoelastically supported sandwich beam

Ranjay Ghosh[†]

Theoretical and Applied Mechanics, Cornell University, Ithaca, New York 14853-1503, USA

Sanjay Dharmavaram[‡] and Kumar Ray^{‡†}

Department of Mechanical Engineering, Indian Institute of Technology, Kharagpur-721302, India

P. Dash^{‡‡}

A.T. - Bidyadharpur Sasam, P.O. Khaira, Dist., Orissa, Balasore-756048, India

(Received November 13, 2003, Accepted November 19, 2004)

Abstract. The parametric dynamic stability of an asymmetric sandwich beam with viscoelastic core on viscoelastic supports at the ends and subjected to an axial pulsating load is investigated. A set of Hill's equations are obtained from the non-dimensional equations of motion by the application of the general Galerkin method. The zones of parametric instability are obtained using Saito-Otomi conditions. The effects of shear parameter, support characteristics, various geometric parameters and excitation force on the zones of instability are investigated.

Key words: parametric dynamic instability; viscoelastic core; sandwich beam; viscoelastic supports; zone instability; simple and combination resonances.

1. Introduction

Quite a few researchers have considered the effects of end-flexibilities on the response and stability of beams. In practice, such considerations are important since the ideal end conditions like clamped-free, pinned-pinned, etc. can be seldom achieved. Saito and Otomi (1979) considered the response of viscoelastically supported ordinary beams. The effects of translational and rotational end-flexibilities on natural frequencies of free vibration of Timoshenko beams were investigated by Abbas (1984). Cortinez and Laura (1985) studied the vibration and buckling of non-uniform beams with a rotational restraint at one end and a concentrated mass at the other. The free and forced vibrations of elastically restrained beams were investigated by Maurizi *et al.* (1988). Kar and Sujata

[†] Graduate Student, E-mail: u0me1012@iitian.iitkgp.ernet.in

[‡] Graduate Student, E-mail: u0me3002@iitian.iitkgp.ernet.in

^{‡†} Assistant Professor, Corresponding author, E-mail: raykr@mech.iitkgp.ernet.in

^{‡‡} Ex-research Scholar

(1988) reported the regions of instability for simple parametric resonance of a nonuniform beam with an elastic end support and thermal gradient. The same authors (Kar and Sujata 1990) considered the parametric instability of an elastically restrained cantilever beam. Metrikine and Dieterman (1997) investigated the effect of axial compression on the instability of vibration of a uniformly moving mass on a beam on viscoelastic foundation. Zheng *et al.* (2000) investigated the instability of a similar 'moving load system' with the load approximated as a single-axle mass-spring-damper system. The authors showed that instability occurs for lower masses as compression axial force increases. Metrikine and Verichev (2001) introduced a two degrees of freedom load and approximated the rail as a Timoshenko beam. They have observed that under these approximations, larger mass of the load lowers the velocity at which instability is observed. The same authors (Verichev and Metrikine 2003) have considered the effect of periodic variations of the foundation stiffness on instability. The dynamic stability of a rotating sandwich beam using the finite element method has been studied by Lin and Chen (2002, 2003).

Beams with viscoelastic core are very popular in reducing structural damping (Habip 1965). However, the effect of viscoelastic supports on the stability of such structures has not been studied previously. In the present study, an attempt has been made to incorporate the viscoelastic nature of real supports to study the stability of asymmetric sandwich beams subjected to an axial pulsating load. This situation may occur in any practical application where a beam is not supported ideally at the ends. The effects of various non-dimensional parameters on the zones of parametric instability are investigated.

2. Formulation of the problem

Fig. 1 shows the system configuration. The top layer of the beam is made of an elastic material of thickness $2h_1$ and Young's modulus E_1 and bottom layer is made of an elastic material of thickness $2h_3$ and Young's modulus E_3 . The core is made of a linearly viscoelastic material with shear modulus $G_2^* = G_2(1 + j\eta)$ where G_2 is the in phase shear modulus, η is the core loss factor and $j = \sqrt{-1}$. The core has a thickness of $2h_2$. The beam is restrained by translational and rotational springs. The moduli of the springs are given as $k_{r1}^* = k_{r1}(1 + j\eta_{r1})$, $k_{r2}^* = k_{r2}(1 + j\eta_{r2})$, $k_{t1}^* =$

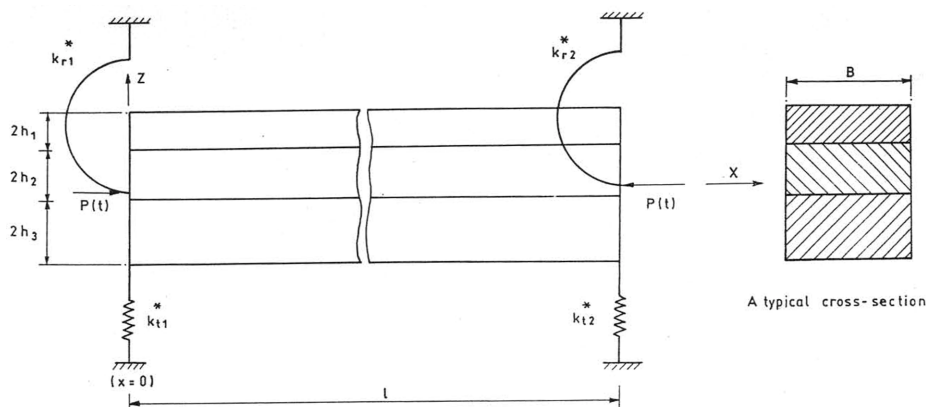


Fig. 1 System configuration

$k_{r1}(1 + j\eta_{r1})$, $k_{r2}^* = k_{r2}(1 + j\eta_{r2})$, subscripts t and r refer to the translational and rotational springs respectively, η etc being the spring loss factors (Fig. 1).

The beam is subjected to pulsating axial loads $P(t) = P_0 + P_1 \cos\omega t$, acting along the undeformed axis as shown. Here ω is the frequency of the applied load, P_0 and P_1 are respectively the static and dynamic load amplitudes and t is the time. The following assumptions are made for deriving the equations of motion:

1. The deflections of the beam are small and the transverse deflection $w(x, t)$ is the same for all points of a cross-section.
2. The layers are perfectly bonded so that displacements are continuous across interfaces, that is, no slipping conditions prevail between the elastic and viscoelastic layers at their interfaces.
3. The elastic layers obey Euler-Bernoulli beam theory.
4. Damping in the viscoelastic core is predominantly due to shear.
5. Bending and the extensional effects in the core are negligible.
6. Extension and rotary inertia effects are negligible.

The expressions for potential energy, kinetic energy and work done are as follows

$$V = \frac{1}{2}E_1A_1\int_0^L u_{1,x}^2 dx + \frac{1}{2}E_3A_3\int_0^L u_{3,x}^2 dx + \frac{1}{2}(E_1I_1 + E_3I_3)\int_0^L w_{,xx}^2 dx + \frac{1}{2}G_2^*A_2\int_0^L \gamma_2^2 dx + \frac{1}{2}k_{t1}^*w^2(0, t) + \frac{1}{2}k_{t2}^*w^2(L, t) + \frac{1}{2}k_{r1}^*\gamma_2^2(0, t) + \frac{1}{2}k_{r2}^*\gamma_2^2(L, t) \tag{1}$$

$$T = \frac{1}{2}m\int_0^L w_{,t}^2 dx \tag{2}$$

$$W_P = \frac{1}{2}\int_0^L P(t)w_{,x}^2 dx \tag{3}$$

where, u_1 and u_3 are the axial displacements in the top and bottom layers and γ_2 is the shear in the middle layer given by $\gamma_2 = \frac{u_1 - u_3}{2h_2} - \frac{cw_{,x}}{2h_2}$. u_3 is eliminated using the Kerwin assumption (Kerwin 1959).

The application of the extended Hamilton's principle

$$\delta \int_{t_1}^{t_2} (T - V + W_P) dt = 0$$

gives the following system of equations of motion

$$mw_{,tt} + (E_1I_1 + E_3I_3)w_{,xxxx} - \left(\frac{G_2^*A_2c^2}{(2h_2)^2} - P(t) \right) w_{,xx} + \frac{G_2^*A_2c(1 + \alpha)}{(2h_2)^2} u_{1,x} = 0 \tag{4}$$

$$(E_1A_1 + \alpha^2 E_3A_3)u_{1,xx} - \frac{G_2^*A_2(1 + \alpha)^2}{(2h_2)^2} u_1 + \frac{G_2^*A_2c(1 + \alpha)}{(2h_2)^2} w_{,x} = 0 \tag{5}$$

At $x = 0$, the associated boundary conditions are,

$$(E_1I_1 + E_3I_3)w_{,xxx} - \left(\frac{G_2^*A_2c^2}{(2h_2)^2} - P(t) \right) w_{,x} - k_{t1}^*w + \frac{G_2^*A_2c(1 + \alpha)}{(2h_2)^2} u_1 = 0 \tag{6}$$

or

$$w = 0 \quad (7)$$

$$(E_1 I_1 + E_3 I_3) w_{,xx} + \frac{k_{r1}^* (h_1 + h_3)}{(2h_2)^2} \{ (h_1 + h_3) w_{,x} - (1 + \alpha) u_1 \} = 0 \quad (8)$$

or

$$w_{,x} = 0 \quad (9)$$

$$(E_1 A_1 + \alpha^2 E_3 A_3) u_{1,x} + \frac{k_{r1}^* (1 + \alpha)}{(2h_2)^2} \{ (1 + \alpha) u_1 - (h_1 + h_3) w_{,x} \} = 0 \quad (10)$$

or

$$u_1 = 0 \quad (11)$$

The boundary conditions at $x = l$ are obtained from relations (6) to (11) by replacing k_{r1}^* and k_{r1}^* by k_{r2}^* and k_{r2}^* respectively.

In the above, $w_{,tt} = \frac{\partial^2 w}{\partial t^2}$, $w_{,xx} = \frac{\partial^2 w}{\partial x^2}$ etc. Also, $\alpha = \frac{E_1 A_1}{E_3 A_3}$ where A_1 and A_3 are cross sectional

areas of the top and bottom layer respectively. Moreover, $c = h_1 + 2h_2 + h_3$. I_1 and I_3 are the moments of inertia of the top & bottom layer cross sections about relevant axes.

Also, u_1 is the axial deflection of the middle of top layer. In the following,

$$\bar{w}_{, \bar{t}\bar{t}} = \frac{\partial^2 \bar{w}}{\partial \bar{t}^2}$$

$$\bar{w}_{, \bar{x}} = \frac{\partial \bar{w}}{\partial \bar{x}}$$

$$\bar{f}_j = \frac{d^2 f}{d \bar{t}^2}$$

$$\bar{v}_n = \frac{d^2 v_n}{d \bar{t}^2}$$

etc. Introducing the dimensionless parameters $\bar{x} = x/l$, $\bar{w} = w/l$, $\bar{u}_1 = u_1/l$, $\bar{t} = t/t_0$, where $t_0^2 = ml^4/(E_1 I_1 + E_3 I_3)$, $\bar{\omega} = \omega t_0$, $\bar{P}_0 = (P_0 l^2)/(E_1 I_1 + E_3 I_3)$, $\bar{P}_1 = (P_1 l^2)/(E_1 I_1 + E_3 I_3)$, $\bar{P}(\bar{t}) =$

$\bar{P}_0 + \bar{P}_1 \cos \bar{\omega} \bar{t}$, $g^* = \frac{G_2 h_{21} l_{h1}^2}{E_1 (1 + E_3 h_{31}^3)} = g(1 + j\eta_r)$, g being the shear parameter). $h_{21} = 1/h_{12} = h_2/h_1$,

$h_{31} = h_3/h_1$, $h_{32} = h_3/h_2$, $l_{h1} = l/h_1$, $E_{31} = E_3/E_1$, Eqs. (4) to (11) reduce to,

$$\bar{w}_{,\bar{t}\bar{t}} + \bar{w}_{,\bar{x}\bar{x}\bar{x}\bar{x}} + \left\{ \bar{P}(\bar{t}) - 3g^* \left(1 + \frac{h_{12} + h_{32}}{2} \right)^2 \right\} \bar{w}_{,\bar{x}\bar{x}} + \frac{3}{2} g^* h_{12} l_{h1} \left(1 + \frac{h_{12} + h_{32}}{2} \right) (1 + \alpha) \bar{u}_{1,\bar{x}} = 0 \quad (12)$$

$$\bar{u}_{1,\bar{x}\bar{x}} - \frac{g^*}{4} h_{12}^2 (1 + \alpha) (1 + E_{31} h_{31}^3) \bar{u}_1 + \frac{g^* h_{12}}{2 l_{h1}} (1 + E_{31} h_{31}^3) \left(1 + \frac{h_{12} + h_{32}}{2} \right) \bar{w}_{,\bar{x}} = 0 \quad (13)$$

The non-dimensional boundary conditions at $\bar{x} = 0$ are as follows.

$$\bar{w}_{,\bar{x}\bar{x}\bar{x}} + \left\{ \bar{P}(\bar{t}) - 3g^* \left(1 + \frac{h_{12} + h_{32}}{2} \right)^2 \right\} \bar{w}_{,\bar{x}} - \bar{k}_{r1}^* \bar{w} + \frac{3}{2} g^* h_{12} l_{h1} \left(1 + \frac{h_{12} + h_{32}}{2} \right) (1 + \alpha) \bar{u}_1 = 0 \quad (14)$$

or

$$\bar{w} = 0 \quad (15)$$

$$\bar{w}_{,\bar{x}\bar{x}} - \bar{k}_{r1}^* \frac{(1 + h_{31})}{l_{h1}} \bar{w}_{,\bar{x}} - \bar{k}_{r1}^* (1 + \alpha) \bar{u}_1 = 0 \quad (16)$$

or

$$\bar{w}_{,\bar{x}} = 0 \quad (17)$$

$$\bar{u}_{1,\bar{x}} + \frac{1}{3} \bar{k}_{r1}^* \frac{(1 + E_{31} h_{31}^3)}{l_{h1} (1 + h_{31})} (1 + \alpha) \bar{u}_1 - \frac{2}{3} \bar{k}_{r1}^* \frac{(1 + E_{31} h_{31}^3)}{l_{h1}^2} \bar{w}_{,\bar{x}} = 0 \quad (18)$$

$$\bar{u}_1 = 0 \quad (19)$$

In the above, $\bar{k}_{r1}^* = \bar{k}_{r1} (1 + J\eta_{r1}) = \frac{k_{r1}^* l^3}{(E_1 I_1 + E_3 I_3)}$, $\bar{k}_{r1} = \bar{k}_{r1} (1 + J\eta_{r2}) = \frac{k_{r1}^* (h_1 + h_3) l^2}{4h_2^2 (E_1 I_1 + E_3 I_3)}$, η_{r1} and

η_{r1} respectively being the non-dimensional \bar{k}_{r1}^* and \bar{k}_{r1} are the non-dimensional spring parameters for the springs at $\bar{x} = 0$.

The boundary conditions at $\bar{x} = 1$ can be obtained from (14) to (19) by replacing \bar{k}_{r1}^* and \bar{k}_{r1} by \bar{k}_{r2}^* and \bar{k}_{r2} , respectively, where \bar{k}_{r2}^* and \bar{k}_{r2} are defined similar to \bar{k}_{r1}^* and \bar{k}_{r1} .

3. Approximate solutions

Approximate solutions of (12) and (13) are assumed as

$$\bar{w} = \sum_{i=1}^{i=N} w_i(\bar{x}) f_i(\bar{t}) \quad (20)$$

$$\bar{u}_1 = \sum_{k=N+1}^{k=2N} u_{1k}(\bar{x}) f_k(\bar{t}) \quad (21)$$

where f_r ($r = 1, 2, \dots, 2N$) are the generalized coordinates and $w_i(\bar{x})$, $u_{1k}(\bar{x})$ are the shape functions to be so chosen as to satisfy as many of the boundary conditions as possible (Leipholz 1987). For

the above mentioned boundary conditions, the shape functions chosen are of the following general form (Kar and Ray 1995),

$$w_i(\bar{x}) = a_0\bar{x}^{i+1} + a_1\bar{x}^{i+2} + a_2\bar{x}^{i+3} \quad (22)$$

$$u_{ik}(\bar{x}) = b_0\bar{x}^{\bar{k}} + b_1\bar{x}^{\bar{k}+1} \quad \text{where} \quad \bar{k} = k - N \quad (23)$$

for $i = 1, 2, \dots, N$ and $k = N + 1, N + 2, \dots, 2N$. The specific values of coefficients a_0, a_1, a_2, b_0 and b_1 are obtained by substituting Eqs. (22) and (23) into Eqs. (14), (16) and (18) and arbitrarily setting a_0 and b_0 (here $a_0 = b_0 = 1$).

Substitution of (20) and (21) in the non-dimensional equations of motion and application of general Galerkin method (Leipholz 1987), leads to the following matrix equations of motion:

$$[m]\{\ddot{f}_j\} + [k_{11}]\{f_j\} + [k_{12}]\{f_l\} = \{0\} \quad (24)$$

$$[k_{22}]\{f_l\} + [k_{21}]\{f_j\} = \{0\} \quad (25)$$

For $j = 1, 2, \dots, N$ and $l = (N + 1), \dots, 2N$, the various matrix elements are given by,

$$m_{ij} = \int_0^1 w_i w_j d\bar{x} \quad (26)$$

$$k_{11ij} = \int_0^1 w_i'' w_j'' d\bar{x} + \left[3g^* \left(1 + \frac{h_{12} + h_{32}}{2} \right) - \bar{P}(\bar{t}) \right] \int_0^1 w_i' w_j' d\bar{x} + \bar{k}_{i1}^* w_i(0) w_j(0) + \bar{k}_{i2}^* w_i(1) w_j(1) + \bar{k}_{r1}^* w_i'(0) w_j'(0) + \bar{k}_{r2}^* w_i'(1) w_j'(1) \quad (27)$$

$$k_{12ik} = -\frac{3}{2} g^* l_{h1} h_{12} (1 + \alpha) \left(1 + \frac{h_{12} + h_{32}}{2} \right) \int_0^1 w_i' u_{1k} d\bar{x} + \bar{k}_{r1}^* u_{1k}(0) w_i'(0) + \bar{k}_{r2}^* u_{1k}(1) w_i'(1) \quad (28)$$

$$k_{22kl} = 3l_{h1}^2 \frac{1 + \alpha^2 E_{31} h_{31}}{1 + E_{31} h_{31}} \int_0^1 u_{1k}' u_{1l}' d\bar{x} + \frac{3}{4} g^* l_{h1}^2 h_{12}^2 (1 + \alpha)^2 \int_0^1 u_{1k} u_{1l} d\bar{x} + \bar{k}_{r1}^* u_{1k}(0) u_{1l}(0) + \bar{k}_{r2}^* u_{1k}(1) u_{1l}(1) \quad (29)$$

Also, $[k_{21}] = [k_{12}]^T$. From (25), $\{f_l\} = -[k_{22}]^{-1}[k_{21}]\{f_j\}$. Substitution of this in (24) leads to,

$$[m]\{\ddot{f}\} + [k]\{f\} - \bar{P}_1 \cos(\bar{\omega}\bar{t})[H]\{f\} = \{0\} \quad (30)$$

where $\{f\} = \{f_1, \dots, f_N\}^T$, $H_{ij} = \int_0^1 w_i' w_j' d\bar{x}$ and $[k] = [T_{11}] - [k_{12}][k_{22}]^{-1}[k_{12}]^T$ with,

$$T_{11ij} = \int_0^1 w_i'' w_j'' d\bar{x} + \left[3g^* \left(1 + \frac{h_{12} + h_{32}}{2} \right) - \bar{P}_0 \right] \int_0^1 w_i' w_j' d\bar{x} + \bar{k}_{i1}^* w_i(0) w_j(0) + \bar{k}_{i2}^* w_i(1) w_j(1) + \bar{k}_{r1}^* w_i'(0) w_j'(0) + \bar{k}_{r2}^* w_i'(1) w_j'(1) \quad (31)$$

4. Regions of instability

Let $[L]$ be the modal matrix of $[m]^{-1}[k]$. Then by the introduction of the linear coordinate transformation, $\{f\} = [L]\{v\}$, $\{v\}$ being a new set of generalized coordinates yields,

$$\{\ddot{v}\} + [\omega_n^2]\{v\} + \bar{P}_1 \cos(\bar{\omega}t)[B]\{v\} = \{0\} \quad (32)$$

where $[\omega_n^2]$ is a spectral matrix corresponding to $[m]^{-1}[k]$ and $[B] = -[L]^{-1}[m]^{-1}[H][L]$. Eq. (32) can be written as,

$$\ddot{v}_n + \omega_n^2 v_n + \bar{P}_1 \cos(\bar{\omega}t) \sum_{m=1}^{m=N} b_{nm} u_n = 0, \quad n = 1, 2, \dots, N \quad (33)$$

Eq. (32) represents a system of N coupled Hill's equations with complex coefficients. Here, ω_n and b_{nm} are complex quantities, given by,

$$\omega_n = \omega_{n,R} + J\omega_{n,I} \quad (34)$$

$$b_{nm} = b_{nm,R} + Jb_{nm,I} \quad (35)$$

The boundaries of the region of instability of simple and combination resonances are obtained using the following conditions by Saito & Otomi (1979).

4.1 Case(A): Simple resonance

In this case, the regions of instability are given by,

$$\left| \frac{\bar{\omega}}{2} - \omega_{\mu,R} \right| < \frac{1}{4} \sqrt{\frac{\bar{P}_1^2 (b_{\mu\mu,R}^2 + b_{\mu\mu,I}^2)}{\omega_{\mu,R}^2} - 16\omega_{\mu,I}^2} \quad (36)$$

when damping is present and,

$$\left| \frac{\bar{\omega}}{2} - \omega_{\mu,R} \right| < \frac{1}{4} \frac{|\bar{P}_1 b_{\mu\mu,R}|}{\omega_{\mu,R}} \quad (37)$$

for the undamped case for $\mu = 1, 2, \dots, N$.

4.2 Case(B): Combination resonance of the sum type

This type of resonance occurs when $\mu \neq v$; $\mu, v = 1, 2, \dots, N$ and the regions of instability are given by:

$$\left| \frac{\omega}{2} - \frac{1}{2}(\omega_{\mu,R} + \omega_{v,R}) \right| < \frac{\omega_{\mu,I} + \omega_{v,I}}{8\sqrt{\omega_{\mu,I}\omega_{v,I}}} \sqrt{\frac{\bar{P}_1^2}{\omega_{\mu,R}\omega_{v,R}} (b_{\mu v,R} b_{v\mu,R} + b_{\mu v,I} b_{v\mu,I}) - 16\omega_{\mu,I}\omega_{v,I}} \quad (38)$$

for the damped case and,

$$\left| \frac{\bar{\omega}}{2} - \frac{1}{2}(\omega_{\mu,R} + \omega_{\nu,R}) \right| < \frac{\bar{P}_1}{4} \sqrt{\frac{b_{\mu\nu,R} b_{\nu\mu,R}}{\omega_{\mu,R} \omega_{\nu,R}}} \quad (39)$$

for the undamped case.

4.3 Case(C): Combination resonance of the difference type

This type of resonance occurs when $\mu < \nu$, ($\mu, \nu = 1, 2, \dots, N$) and the regions of instability are given by:

$$\left| \frac{\bar{\omega}}{2} - \frac{1}{2}(\omega_{\nu,R} - \omega_{\mu,R}) \right| < \frac{\omega_{\mu,I} + \omega_{\nu,I}}{8\sqrt{\omega_{\mu,I}\omega_{\nu,I}}} \sqrt{\frac{\bar{P}_1^2}{\omega_{\mu,R}\omega_{\nu,R}} (-b_{\mu\nu,R}b_{\nu\mu,R} + b_{\mu\nu,I}b_{\nu\mu,I}) - 16\omega_{\mu,I}\omega_{\nu,I}} \quad (40)$$

for the damped case and

$$\left| \frac{\bar{\omega}}{2} - \frac{1}{2}(\omega_{\nu,R} - \omega_{\mu,R}) \right| < \frac{\bar{P}_1}{4} \sqrt{\frac{-b_{\mu\nu,R}b_{\nu\mu,R}}{\omega_{\mu,R}\omega_{\nu,R}}} \quad (41)$$

for the undamped case.

5. Numerical results and discussion

For relevant values of system parameters, zones of instability of the present study are compared to those of Saito and Otomi (1979) and good agreement was observed. Numerical results were obtained for the viscoelastically supported beam to study the effects of the non-dimensional parameters η , η_{t2} , η_{r2} , k_{t2} , k_{r2} , g , h_{31} , h_{12} , l_{h1} and \bar{P}_0 on the zones of parametric instability. The following parameter values have been taken, unless stated otherwise. $\eta = 0.1$, $\eta_{t1} = \eta_{t2} = 0.1$, $\eta_{r1} = \eta_{r2} = 0.01$, $\bar{k}_{t1} = \bar{k}_{t2} = 1$, $\bar{k}_{r1} = \bar{k}_{r2} = 750$, $l_{h1} = 10$, $g = 0.05$, $\bar{P}_0 = 0.1$, $h_{31} = h_{12} = 1$, $E_{31} = 1$, $\alpha = 1$. In the figures $\omega_{q,R}$ is replaced by ω_q ($q = 1, 2, 3$) for brevity. It must be noted that only the lowest three natural frequencies are taken so that the Euler-Bernoulli assumption is not compromised. To be able to extract meaningful information from the plots, a few basic but vital explanations are in order. The space inside the V-shaped curve is the region of instability. A section of these 3-dimensional plots, by a plane parallel to the $\bar{P}_1 - \bar{\omega}$ plane would give us plots similar to Saito and Otomi (1979). Improvement in stability is indicated by a reduction in the cross-sectional area of the zone and vice versa. The various figures from Fig. 2 onwards are oriented differently for the sake of clarity. Also, Fig. (a) in each Fig. (Except in Figs. 7 and 10), gives a global view of the zones. The other figures (Figs. b,c and d)(except in Figs. 7 and 10) are magnified versions of these zones for clarity. All plots are on a linear scale. Some of the findings are explained without figures. This is because the associated figures would essentially be similar to the ones presented. This is done to keep the number of figures to a minimum.

Fig. 2 shows the effect of η on the zones of instability of the simple resonance. For zones near $2\omega_1$, the stability improves gradually with increasing value of η , until the zones completely disappear. However, for the next two frequencies, the stability first deteriorates till a critical value of η is reached and then continuously improves till unstable zones completely disappear. In a similar

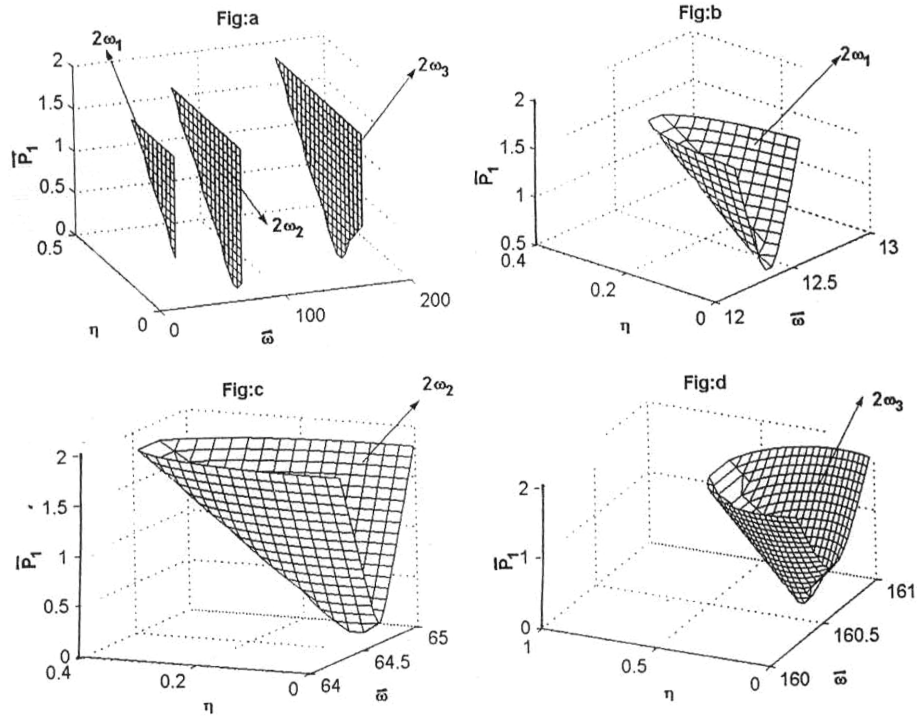


Fig. 2 Zones of simple resonance for η

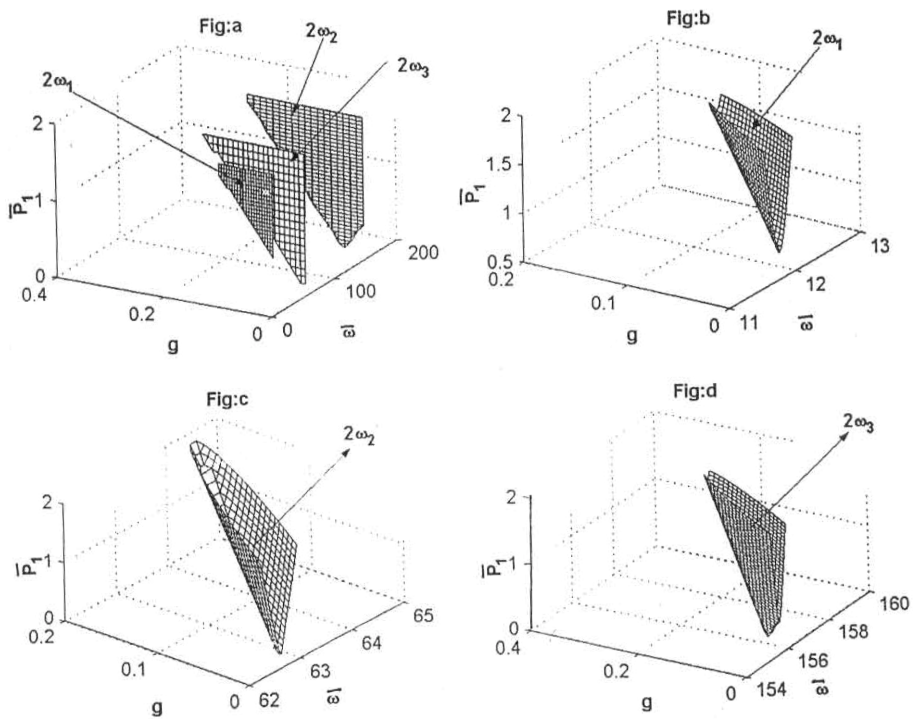


Fig. 3 Zones of simple resonance for g

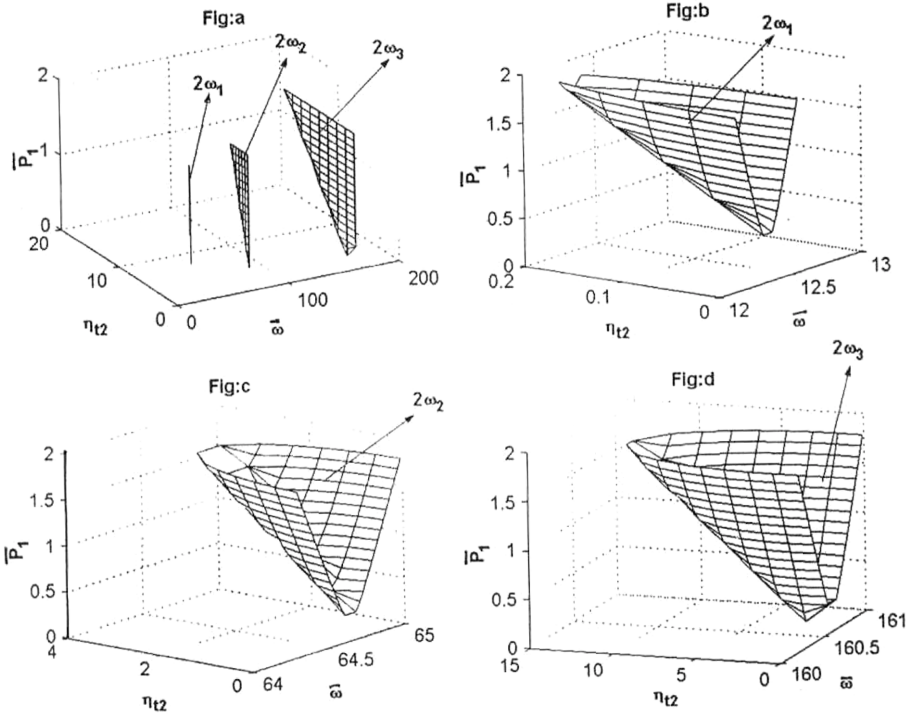


Fig. 4 Zones of simple resonance for η_{12}

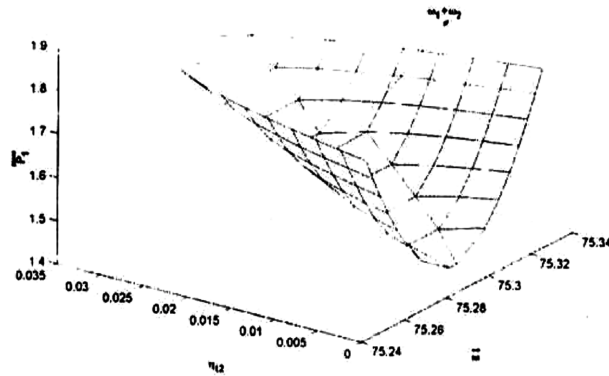


Fig. 5 Zones of combination resonance for η_{12}

fashion, combination resonance was seen to occur near $\omega_1 + \omega_2$, $\omega_1 + \omega_3$ and $\omega_2 + \omega_3$. However, with an increase in η , the zones moved upwards until they disappeared completely (Figures for these not shown). In all cases, zones do not show any shift along the frequency axis.

An increase in the value of g improves the stability in general by shifting the zones vertically upwards. However, in cases of simple resonance shown in Fig. 3, the zones near $2\omega_3$ show an initial worsening in stability before the zones start moving upwards indicating an improvement in stability.

Figs. 4 and 5 show the influence of η_{12} on stability. For simple resonance, for the first two natural frequencies, stability continuously improves with increase in parameter value till complete zone

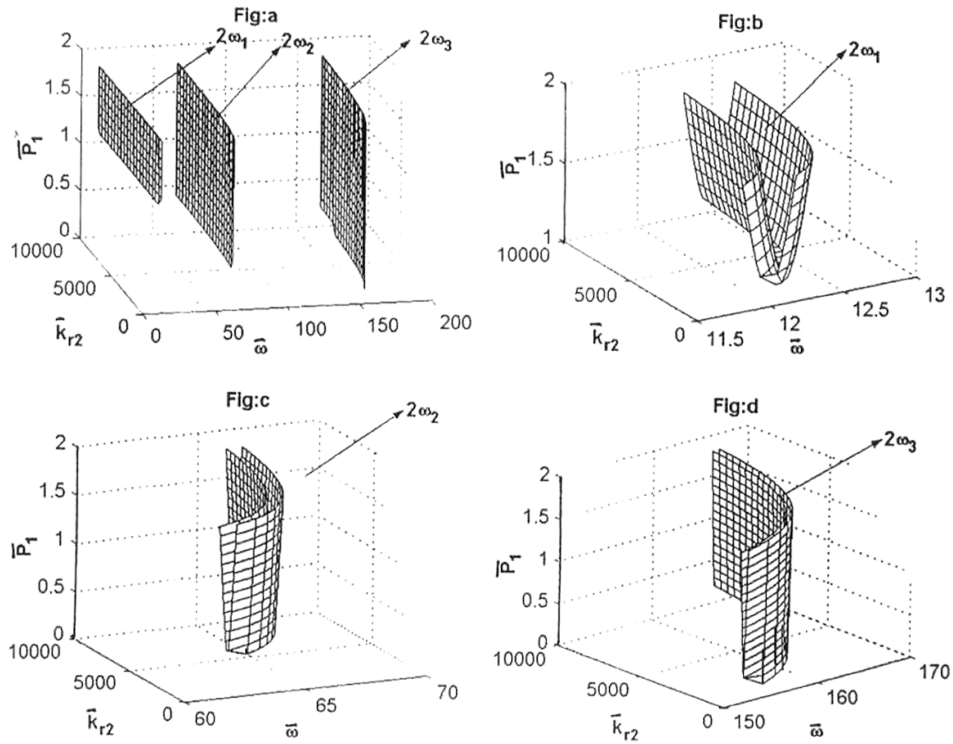


Fig. 6 Zones of simple resonance for \bar{k}_{r2}

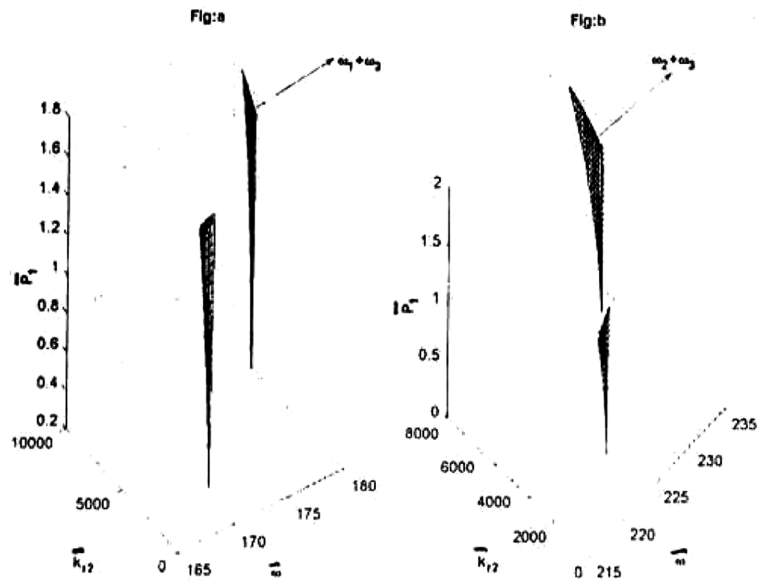


Fig. 7 Zones of combination resonance for \bar{k}_{r2}

disappearance occurs. However, for the zones near $2\omega_3$, the stability first deteriorates and then continues to improve till complete disappearance is observed. Combination resonance is observed near $\omega_1 + \omega_2$ only. Here, stability steadily improves with an increase in parameter value till the zones disappear. In all the above cases, there is no shift along the frequency axes.

Similar behavior was observed for η_{r2} except that no combination resonance appears.

An increase in the value of \bar{k}_{r2} causes the zones to shift vertically upwards and also a little towards higher excitation frequency (figures not given).

The effect of \bar{k}_{r2} on the system stability is studied through Figs. 6 and 7. For simple resonance, the stability worsens for low \bar{k}_{r2} but improves subsequently as zones move up a little. In all cases, the zones move towards higher excitation frequency. In case of combination resonance near $\omega_1 + \omega_3$ and $\omega_2 + \omega_3$, stability improves gradually till the zones disappear at some critical value of the parameter. The zones reappear later and stability gradually improves again till the zones disappear completely. No zones are observed near $\omega_1 + \omega_2$.

Figs. 8 and 9 demonstrate the dependence of the zones of instability on h_{31} . For simple resonance near $2\omega_1$, the zones move continuously upwards for lower values of h_{31} before completely disappearing. They reappear later at higher frequencies and continue to move downwards thereby worsening stability. For simple resonance near $2\omega_2$, the zone monotonically shifts upwards with an increase in the parameter value until it disappears. The zone near $2\omega_3$ initially shifts downwards worsening the stability. Then, it again moves upwards, gradually restoring stability to the system. For combination resonance, stability continues to improve as indicated by a steady vertical rise of zones until complete disappearance, Fig. 9.

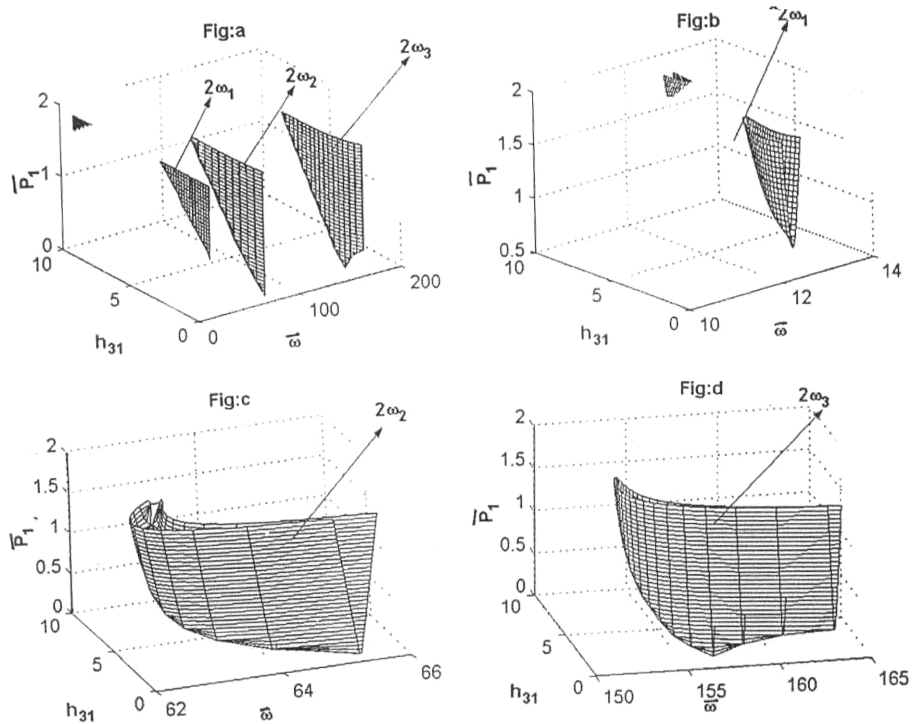


Fig. 8 Zones of simple resonance for h_{31}

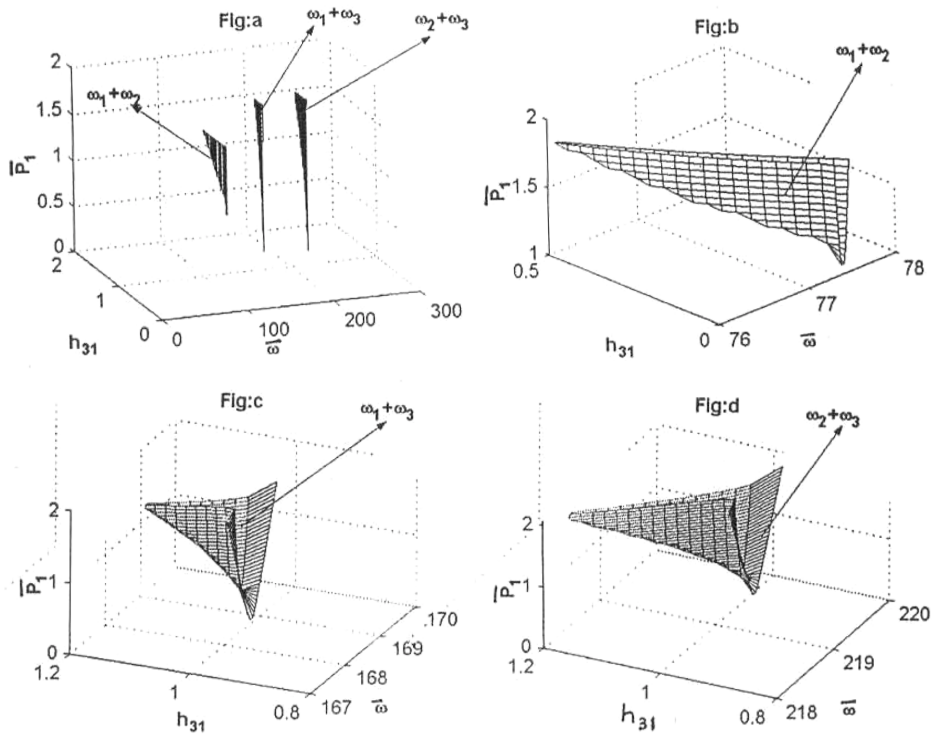


Fig. 9 Zones of combination resonance for h_{31}

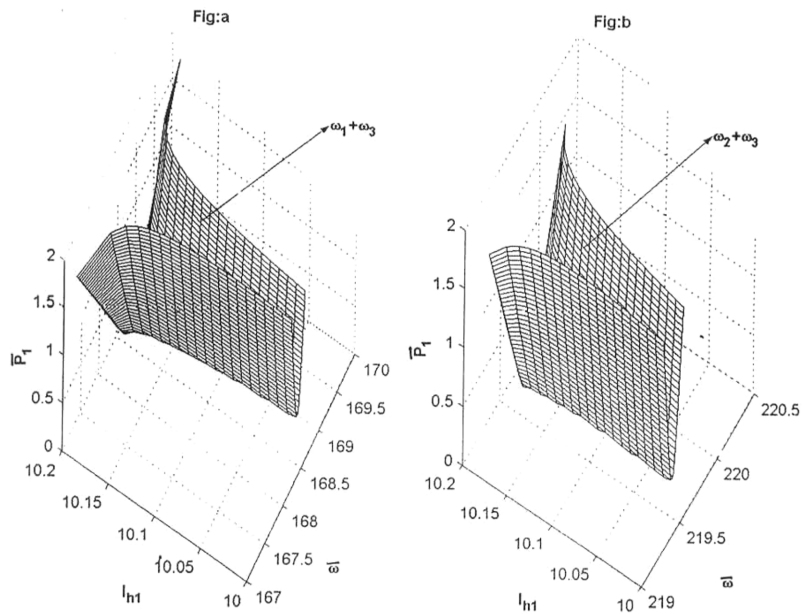


Fig. 10 Zones of combination resonance for l_{h1}

The effect of h_{12} on stability was observed to have the following consequences. For simple resonance, the stability monotonically improves except for the zones near $2\omega_3$ for lower values of h_{12} . For combination resonance, the zones continuously move up before disappearance (figures not given).

The effect of l_{h1} is discussed next. For simple resonance, the zones continually move upwards thus improving the stability except for zones near $2\omega_2$ where stability deteriorates for intermediate values of the parameter. For combination resonance as shown in Fig. 10 near $\omega_1 + \omega_3$ and $\omega_2 + \omega_3$, stability worsens as indicated by the downwards movement and increasing width of the zones. However, no combination resonance is observed near $\omega_1 + \omega_2$.

\bar{P}_0 has the following effect on instability. For simple resonance, the zone width remains constant while the zones show no vertical movement. However, they monotonically shift towards lower frequencies with increase in the value of \bar{P}_0 . For combination resonance near $\omega_2 + \omega_3$, a similar thing happens. No combination resonance occurs near $\omega_1 + \omega_2$ or $\omega_1 + \omega_3$ (figures not given).

6. Conclusions

In the present work, an attempt has been made to include the viscoelastic character of beam supports which is often neglected. The present model can be applied to situations where realistic modelling of supports is necessary in order to predict the dynamical behaviour of the system accurately.

The following are the conclusions drawn from the study.

1. An increase in η steadily improves parametric stability, except for zones near $2\omega_2$ and $2\omega_3$ for low η
2. An increase in η_{12} also steadily improves stability except near $2\omega_3$ for low η_{12}
3. η_{r2} behaves similarly. \bar{k}_{r2} steadily improves stability. Thus stiffer vertical constraints at the ends of the beam results in better parametric stability.
4. The combination zones of instability appear or disappear depending on the value of \bar{k}_{r2} . For certain ranges of parameter value, no such instability occurs. Overall stability improves as \bar{k}_{r2} increases.
5. A higher g is usually better for stability.
6. A higher h_{31} results in better overall stability. Thus, the constraining (top) layer should be thin compared to main (bottom) layer.
7. A higher h_{12} is better for stability.
8. l_{h1} improves the dynamic stability except for small range of values for which combination resonances occur.
9. An increase in \bar{P}_0 shifts the zones of instability towards lower excitation frequencies.
10. Difference type of combination resonance is absent throughout.

References

- Abbas, B.A.H. (1984), "Vibrations of Timoshenko beams with elastically restrained ends", *J. Sound Vib.*, **97**(4), 541-548.
- Cortinez, V.H. and Laura, P.A.A. (1985), "Vibrations and buckling of a non-uniform beam elastically restrained

- against rotation and with concentrated mass at the other”, *J. Sound Vib.*, **99**(1), 144-148.
- Habip, L.M. (1965), “A survey of modern developments in the analysis of sandwich structures”, *Appl. Mech. Review*, **18**, 93-98.
- Kar, R.C. and Ray, K. (1995), “Parametric stability of a pretwisted, three layered symmetric sandwich beam”, *J. Sound Vib.* **182**(4), 591-606.
- Kar, R.C. and Sujata, T. (1988), “Parametric instability of a non-uniform beam with thermal gradient and elastic support journal”, *J. Sound Vib.*, **122**(2), 209-215.
- Kar, R.C. and Sujata, T. (1990), “Parametric instability of an elastic restrained cantilever beam”, *Comput. Struct.*, **34**(3), 469-475.
- Kerwin, E.M. Jr. (1959), “Damping of flexural waves by a constrained viscoelastic layer”, *The J. of the Acoustical Society of America*, **316**, 952-962.
- Leipholz, H. (1987), *Stability Theory*, Wiley, N.Y.
- Lin, C.Y. and Chen, L.W. (2002), “Dynamic stability of rotating composite beams with a viscoelastic core”, *Comp. Struct.*, **58**, 185-194.
- Lin, C.Y. and Chen, L.W. (2003), “Dynamic stability of a rotating beam with a constrained damping layer”, *J. Sound Vib.*, **267**, 209-225.
- Maurizi, M.J., Bambill de Rossit, D.V. and Laura, P.A.A. (1988), “Free and forced vibrations of beams elastically restrained against translation and rotation at the ends”, *J. Sound Vib.*, **120**(3), 626-630.
- Metrikine, A.V. and Dieterman, H.A. (1997), “Instability of vibrations of a mass moving uniformly along an axially compressed beam on a viscoelastic foundation”, *J. Sound Vib.*, **201**(5), 567-576.
- Metrikine, A.V. and Verichev, S.N. (2001), “Instability of vibrations of a moving two mass oscillator on a flexibly supported Timoshenko beam”, *Arch. of Appl. Mech.*, **71**(9), 613-624.
- Saito, H. and Otomi, K. (1979), “Parametric response of viscoelastically supported beams”, *J. Sound Vib.*, **63**(2), 169-178.
- Verichev, S.N. and Metrikine, A.V. (2003), “Instability of vibrations of a mass that moves uniformly along a beam on a periodically homogeneous foundation”, *J. Sound Vib.*, **260**(5), 901-925.
- Zheng, D.Y., Au, F.T.K. and Cheung, Y.K. (2000), “Vibration of vehicle on compressed rail on viscoelastic foundation”, *J. Engg. Mech.*, ASCE, **126**(11), 1141-1147.